

HYDROPHOBIZATION OF BLEACHED SOFTWOOD KRAFT FIBERS VIA ADSORPTION OF ORGANO-NANOCLAY

Jieming Chen and Ning Yan*

Montmorillonite clay particles that had been prepared with an alkyl-ammonium surfactant were used to modify the moisture-sensitivity of bleached softwood kraft fibers through solvent exchange and adsorption methods. Moisture absorption and water uptake of the wood pulp fibers were significantly lower after the organo-nano clay treatment. Thermal stability, surface energy, and surface morphology of the treated fibers were characterized using Thermogravimetric Analysis (TGA), Inverse Gas Chromatography (IGC), Scanning Electron Microscopy-Energy Dispersive X-ray Analysis (SEM-EDX), and Transmission Electron Microscopy (TEM) imaging. The Fourier Transform Infrared (FT-IR) spectral characteristics of the treated fibers were obtained to better understand the modified surface functional groups of the treated fibers. The treated bio-fibers had nano-scale surface roughness and a much reduced surface energy. The contact angle of water on the treated fiber mat was found to be higher than 160°. The thermal stability of the treated fibers was not affected by the modification.

Keywords: Bio-fibers; Nanoparticle; Surface modification; Clay, Adsorption

Faculty of Forestry, University of Toronto, 33 Willcocks Street, Toronto, ON, Canada M5S 3B3;

* Corresponding author: ning.yan@utoronto.ca

INTRODUCTION

Cellulose is a linear polymer consisting of D-glucose units linked via β , 1-4 glucosidal bonds. As a renewable, abundant, and environmentally-friendly bio-based material, cellulose fibers are increasingly used for a wider range of applications. However, due to the existence of a significant amount of accessible hydroxyl groups at the internal and external fiber surfaces, cellulose fibers are hydrophilic. As a result, the high moisture sensitivity and poor dimensional stability of the cellulosic fibers have significantly limited their utilization.

Several studies have shown that it is possible to modify the cellulose fiber surfaces to increase fiber surface hydrophobicity. Some have obtained superhydrophobic surfaces after modification (Nystrom *et al.* 2006, 2009; Li *et al.* 2010; Yang and Deng 2008; Hu *et al.* 2009; Goncalves *et al.* 2008). Superhydrophobic surfaces have a water contact angle (CA) higher than 150° and a low CA hysteresis (Nystrom *et al.* 2009). Due to their potential applications in areas such as self-cleaning surfaces (Nakajima *et al.* 2001; Zhang and Shi 2008), superhydrophobic surfaces have attracted significant research interest worldwide. Additionally, it was found that appropriate types of surface roughness attributes are important for achieving the superhydrophobicity (Youngblood and McCarthy 1999; Callies and Quere 2005).

To render cellulose fiber hydrophobic, the fibers have to be modified chemically and/or physically (Jin *et al.* 2011; Lindström *et al.* 2008; Bessadok *et al.* 2007; Khalil *et al.* 2001). Research has shown that a chemical modification process, such as the one reported by Nystrom *et al.* (2009) that consisted of grafting glycidyl methacrylate to the hydroxyl groups and post-functionalization to obtain surface superhydrophobicity, was difficult to control and caused degradation in mechanical performance of the fibers. Meanwhile, layer-by-layer (LbL) deposition technique, combined with a post-functionalization process, was one of the frequently used modification methods for obtaining superhydrophobic cellulose fiber surfaces. For example, SiO₂ nano-particles were deposited on the cellulose fiber surfaces using LbL followed by post-functionalization using fluorosiloxane that resulted in superhydrophobic surfaces (Yang and Deng 2008). Cellulose fiber surfaces were also plated with nanoclays via LbL assembly. The plated fibers had reduced flocculation and increased compatibility between the cellulose fibers and a plastic matrix (Lindström *et al.* 2008). However, the modification of a cellulose fiber surface using the LbL technique is a multi-step process involving the usage of polyelectrolytes to transform cellulose fibers' surface charge to achieve electrostatic adsorption. Using these techniques, a large number of layers usually have to be deposited on the fiber surfaces in order to achieve the desired properties.

On the other hand, cellulose fibers are routinely sized during the papermaking process to enhance their hydrophobicity (Yang and Deng 2000; Ishida 1994; Clapperton and Henderson 1947). By utilizing sizing agents such as alkyl ketene dimer (AKD), paper/fibers also demonstrated superhydrophobic characteristics (Quan *et al.* 2009; Balu *et al.* 2008). However, in order to make paper/fibers superhydrophobic, other treatments are needed in addition to the use of the sizing agent, such as plasma treatment and supercritical CO₂ expansion.

Meanwhile, nanoclays, such as Cloisite Na and Cloisite 93A (Southern Clay Company, USA), have been well studied for their applications in nanocomposites (Peeterbroeck *et al.* 2005; Yoon *et al.* 2007). Some nanoclays have been shown to significantly reduce the moisture sensitivity of the composites (Kim *et al.* 2005; Choudalakis and Gotsis 2009; Lei *et al.* 2007). Because nanoclays have excellent barrier properties, they can significantly reduce the permeability of moisture and gas into the composites.

In this paper, a simple modification method of depositing hydrophobic organo-nanoclays on cellulose fiber surfaces through solvent exchange technique was explored. The solvent exchange process allowed hydrophilic kraft pulp fibers to disperse well in non-polar organic solvents. It was hypothesized that by depositing the nanoclays directly on the fiber surfaces, it could reduce moisture and water uptake of the fibers by blocking the accessibility to the hydroxyl groups on the external and internal fibers surface and by deterring moisture and water absorption through increased path tortuosity. Properties such as thermal stability, surface energy, nanoclay particle distribution, moisture absorption, and water uptake of the treated fibers were measured and compared with the untreated fibers. The efficacy of the treatment method for enhancing dimensional stability of the fibers is considered.

EXPERIMENTAL

Materials

Nanoclays

Cloisite Na is a type of natural montmorillonite clay, while Cloisite 93A is referred to as an organo-nanoclay derived from ion exchanging the montmorillonite clay with alkyl ammonium cation (Southern Clay Products, Inc. USA). Cloisite 93A is composed of an inorganic interlayer and an organic outer layer. Due to the long alkyl chains of 16-18 carbon atoms of the nanoclay, Cloisite 93A is hydrophobic (Peeterbroeck *et al.* 2005), and it can only be exfoliated in organic solvents. Table 1 gives the moisture absorption of these two types of nanoclays. The moisture absorption tests were carried out by measuring the weight gain of the clays (compared to oven-dry clay weight) under the test condition of being stored under 95% relative humidity at 25°C for 24 hours in a moisture chamber (Constant Temperature Control Ltd. Canada). The data reported was the average of three replicate tests. Since Cloisite 93A absorbs a significantly lower amount of moisture, it was used to treat the fibers subsequently.

Table 1. Moisture Absorption of the Nanoclays

Type of Nanoclay	Moisture Absorption (wt.%)
Cloisite Na	17.4 ± 0.4
Cloisite 93A	2.6 ± 0.1

Cellulose fibers

Fully bleached softwood kraft pulp fibers (Domtar Inc., Canada) were used in this study. The kraft fibers had an arithmetical average fiber length of 1.15 mm (with a standard deviation of 0.86 mm) and an average fiber width of 24.2 µm (with a standard deviation of 10.0 µm), as measured by using a HiRes Fiber Quality Analyzer (FQA) (Optest Equipment Inc. Canada). The cellulose content was higher than 99%.

Other chemicals, such as toluene and acetone, were purchased from Caledon Company and used without any further purification.

Methods

Preparation of organo-nanoclay treated kraft pulp fibers

Kraft pulp fiber surfaces were first modified by a solvent exchange process, where they were washed several times by acetone, followed by toluene. A calculated amount of organo-nanoclay, Cloisite 93A, was exfoliated in 1000 mL of toluene according to the desired clay concentration. The solvent-exchanged kraft fibers were then added into the clay/toluene solution and stirred for 2 hours. Afterwards, the kraft fibers were filtered first and washed three times with a small amount of toluene prior to any measurements. Clay adsorption isotherm was prepared by treating the fibers in different concentrations of organo-nanoclays dispersed in toluene at room temperature. The organo-nanoclay concentration in toluene was expressed as weight percentage (wt.%) of organo-nanoclays relative to 1 g of the oven-dried kraft fibers. Clay content adsorbed on

the kraft fibers was expressed in a similar manner. Solvent-exchanged kraft fibers without clay-treatment were used as controls for comparison.

Adsorbed clay content

The clay content adsorbed on the kraft fibers was measured in a Muffle furnace (Thermolyne Corporation, USA) by burning the oven-dried, clay-treated and untreated, kraft fibers for 2 hours at 800°C. Weight of the residual ash was then converted to weight percentage of organo-nanoclays on fibers by using the following equations:

$$\begin{aligned} \text{Weight of ash, } W_r &= W_f \cdot W_c \cdot A_c + W_f \cdot (1 - W_c) \cdot A_f \\ &= W_f \cdot A_f + W_f \cdot W_c \cdot (A_c - A_f) \end{aligned} \quad (1)$$

Weight percentage of clays on fibers, W_c , was obtained from equation (1) as follows:

$$W_c = \left(\frac{W_r}{W_f (A_c - A_f)} - \frac{A_f}{A_c - A_f} \right) \times 100 \quad (2)$$

where, W_r and W_f are the weight of the treated fibers after and before burning, respectively. W_c is the weight percentage of clay on 1 g of oven-dried organo-nanoclay treated kraft fibers. A_c and A_f are the ash weights of 1 g of oven-dried clay and 1 g of oven-dried fibers, respectively. A_c and A_f are known by testing clay and kraft fibers separately in a muffle furnace under the same conditions. All weights were measured by an analytical balance to the precision of 0.1 mg. The data reported were the average of three replicate tests.

Moisture absorption experiments

Moisture absorption was tested in a moisture chamber that was kept at 85% relative humidity and 25°C. At predetermined time intervals, samples were weighed in the moisture chamber using an analytical balance. The amount of moisture absorbed was expressed as the percentage of weight gain, which was calculated using the following equation,

$$\text{Weight gain\%} = \frac{W_t - W_0}{W_0} \times 100 \quad (3)$$

where, W_0 is the initial weight of the oven-dried fibers, while W_t is the weight of the fibers at a given time t . For the organo-nanoclay treated fibers, normalized weight gain is also calculated using the equation below to account for the fact that the actual cellulose fiber mass is reduced in the clay-treated fibers due to the presence of clay. The data reported were the average of three replicate tests.

$$\text{Normalized weight gain \%} = \frac{W_t - W_0}{W_0 (1 - W_c)} \times 100 \quad (4)$$

Moisture absorption of the kraft fibers treated with 10%, 15%, and 20% (all in terms of wt.%) of organo-nanoclays in toluene solutions was measured, and the solvent-exchanged

kraft fibers were tested as the control. All fibers were oven dried before testing and kept in a desiccator while being cooled to the room temperature.

Water uptake experiments

The water uptake amount by the treated and untreated kraft fibers was measured by submerging the fibers in distilled water at room temperature. Fibers were placed in a permeable sample net. At pre-determined time intervals, samples were taken out of water for weight measurement until water-uptake amount reached saturation. Prior to weight measurement, surface water was carefully removed from the samples by blotting with tissue paper. Care was taken to ensure the manual blotting process was kept as consistent as possible. The water uptake amount of the fibers was also expressed as a percentage of weight gain and was calculated using equations (3) and (4). The data reported were the average of six replicate tests.

Water contact angle of organo-nanoclay treated kraft fibers

In order to get a comparatively flat surface for performing the contact angle measurement, treated fibers in toluene solution were poured onto a filter paper after the treatment and were carefully removed as a fiber mat. After the fiber mat was dry, the water contact angle of the mat surface was measured using a Mu-Check Star (Mitutoyo, Japan) instrument with a zoom lens at 7 times amplification. 5 µL of distilled water were placed onto the fiber mat surface using a syringe prior to the contact angle measurement. A camera attached to the lens was used to acquire the droplet images used for analysis.

IGC measurement

Inverse gas chromatography (IGC, Clarus 500 Gas Chromatography, Perkin Elmer, USA), a vapor adsorption measurement for characterizing surface energy, was used for comparing surface energy of the organo-nanoclay treated fibers with that of the untreated fibers. Both the injection and detector temperatures were at 150°C. Helium gas was used as the carrier and the flow rate was around 10 mL/min. The oven dried fiber-filled copper column of 2.5 mm in diameter and 33 cm in length was conditioned in a chromatograph oven at 60°C overnight purged with helium to remove moisture prior to IGC measurements.

Table 2. Properties of the Probes Used in the IGC Measurement
(TZE and Gardner 2001)

Probes	Area covered by adsorbed molecules, $a (10^{-20} m^2)$	Dispersive Energy, $\gamma_L^d (mL/m^2)$	Specific Characteristic
n-Hexane	51.5	18.4	Neutral
n-Heptane	57	20.3	Neutral
n-Octane	63	21.3	Neutral
n-Nonane	69	22.7	Neutral
n-Decane	75	23.9	Neutral

Table 2 summarizes the probes used for the IGC tests and their properties. The probes were HPLC-grade alkanes, ranging from n-hexane to n-decane. A probe solution

(0.1 μL) was injected into the column. The retention time of the probe was recorded. Methane gas was used as the control. Before testing the probes, methane was injected until the signal was stabilized. Three injections were made for each probe at 60°C, 70°C, and 80°C, respectively.

The retention time of the probe, passing through the column of the fibers, can be converted to the net specific retention volume by use of the following equation,

$$V_g = \frac{273 \cdot 15}{TW} Q(t_r - t_m) \quad (5)$$

where V_g is the net specific retention volume (mL/g), T is the column temperature (K), W is the weight of the fibers packed in the column (g), Q is the flow rate (mL/min) of the carrier gas, t_r is the retention time of the probe (min), and t_m is the retention time of methane (min).

The dispersive component of the surface energy (DCSE) at the column temperature was determined from the following equation,

$$\gamma_s^d = \left(\frac{RT \ln V_g}{a(\gamma_L^d)^{1/2}} \cdot \frac{1}{2N} \right)^2 \quad (6)$$

where, γ_s^d is the DCSE of the fiber (mJ/m^2), R is the gas constant ($8.3145 \text{ J K}^{-1} \text{ mol}^{-1}$), γ_L^d is the dispersive component of the surface energy of the probe (mJ/m^2), N is the Avogadro number ($6.0221 \times 10^{23} \text{ mol}^{-1}$), and a is the area covered by an adsorbed probe molecule (m^2). The quantity $RT \ln V_g / a(\gamma_L^d)^{1/2}$ can be derived from the slope of the curve by plotting $RT \ln V_g$ versus $a(\gamma_L^d)^{1/2}$ for a series of alkane probes at a given temperature.

Other measurements

Thermal stability of the treated and untreated fibers was measured using a Thermal Gravimetric Analyzer (TGA) (Q500, TA Instruments, USA). Samples were measured in nitrogen with a heating rate of 10°C/min from room temperature to 750°C. The Fourier Transfer Infrared (FTIR) spectral characteristics were obtained using an FTIR spectrometer (Bruker Tensor 27, USA) with KBr pellets. The testing pellets were prepared by mixing 2 mg of the fiber samples with 200 mg spectroscopic grade KBr. IR spectra in the range of 4000 to 400 cm^{-1} were measured with a resolution of 4 cm^{-1} . The software of the equipment removed the effect of H_2O and CO_2 on the spectra, and normalized the spectrum of each sample. The morphology and distribution of the organo-nanoclays on the fiber surface were measured by Scanning Electron Microscope-Energy Dispersive X-ray Analysis (SEM-EDX) (JSM-840 Scanning Microscope, JEOL, USA) and Transmission Electron Microscope (TEM) (Philips 201 TEM, FEI Company, USA). The specimens for SEM measurements were gold sputter-coated. For acquiring TEM images, fibers were embedded in an epoxy resin prior to being sectioned into 80 nm thickness slices with an ultra-microtome knife.

RESULTS AND DISCUSSION

Adsorption of Organo-Nanoclays on Fibers

The characteristics of the organo-nanoclay adsorption on fibers are shown in Fig. 1. When the concentration of organo-nanoclays increased from 5-wt% to 20-wt% in the treatment solutions, the amount of organo-nanoclays adsorbed on the fibers was increased. Further increase in organo-nanoclay concentration from 20-wt% to 40-wt%

showed a more gradual increase in adsorption, approaching a saturation level. Even though the shape of the adsorption curve resembled a Langmuir isotherm, the organo-nanoclays adsorbed on the fiber surface were primarily in the form of multi-layers. Using other methods, it was reported that approximately 4-wt% of clays could provide 100% coverage of the fiber surfaces (Lindström *et al.* 2007). Examination of the 15-wt% of organo-nanoclay treated fibers showed that the adsorbed organo-nanoclays were in fact of the form of multi-layers of around 0.5 μm in thickness, as shown in the TEM image in Fig. 2b.

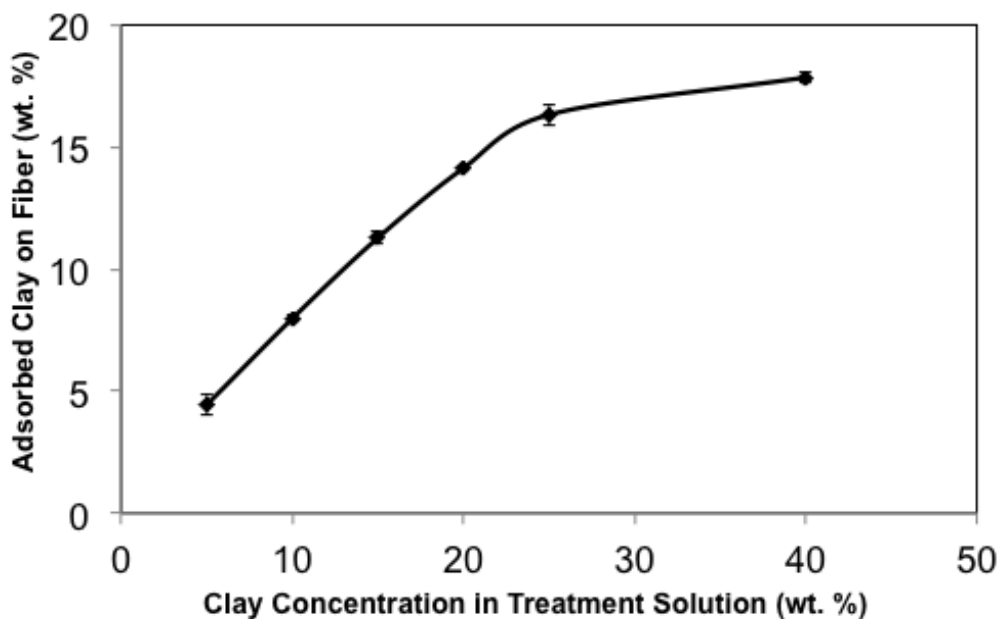


Fig. 1. The amount of organo-nanoclays adsorbed on the fiber surface as a function of different concentrations of organo-nanoclays in the treatment solutions

Figure 3 shows an SEM image of 15-wt% organo-nanoclay treated fiber. To illustrate the distribution of the organo-nanoclays on the fiber surface, a line scan (ten points on the upper line in Fig. 3) was performed with EDX. An intensity distribution plot is superimposed on the image of the fiber. Since silicon is the main constituent in the organo-nanoclay, its presence indicates the clay location on the fiber, and the peak height represents the content of the clay. From Fig. 3, it can be seen that high intensity peaks of silicon appeared around the center of the fiber, near to the fiber pits. This area indicated a higher content of organo-nanoclay, implying that organo-nanoclays might have passed

through the fiber pit and entered into the fiber lumen. In addition, the distribution of organo-nanoclays on the fiber surface was shown to be highly non-uniform.

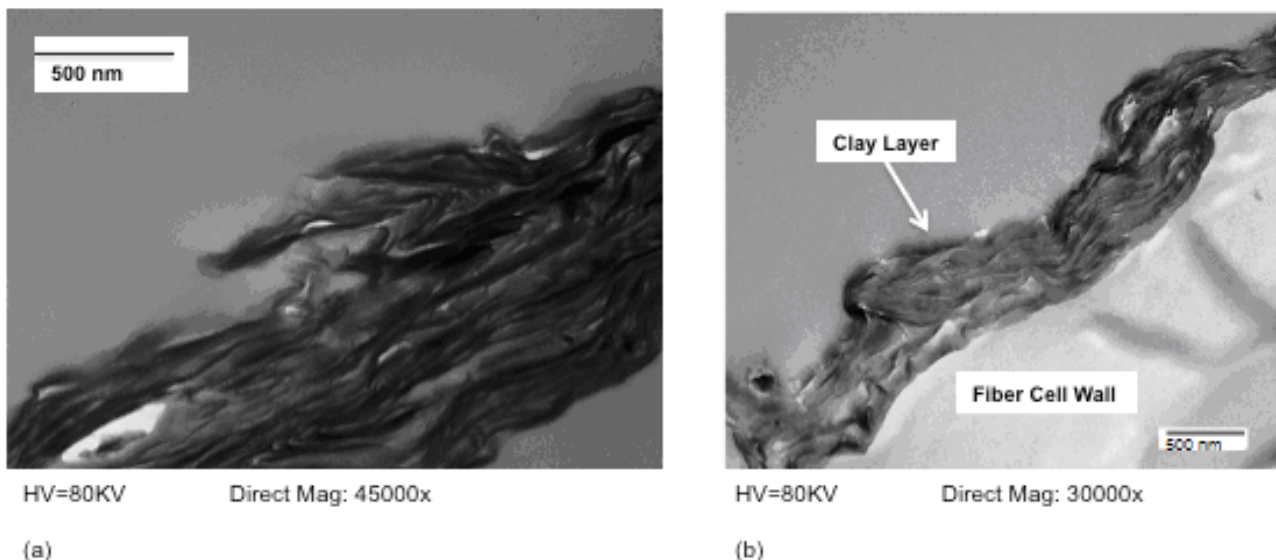


Fig. 2. TEM image of (a) Cloisite 93A organo-nanoclay; (b) cross sectional view of an organo-nanoclay treated fiber showing the Cloisite 93A layer on the fiber surface

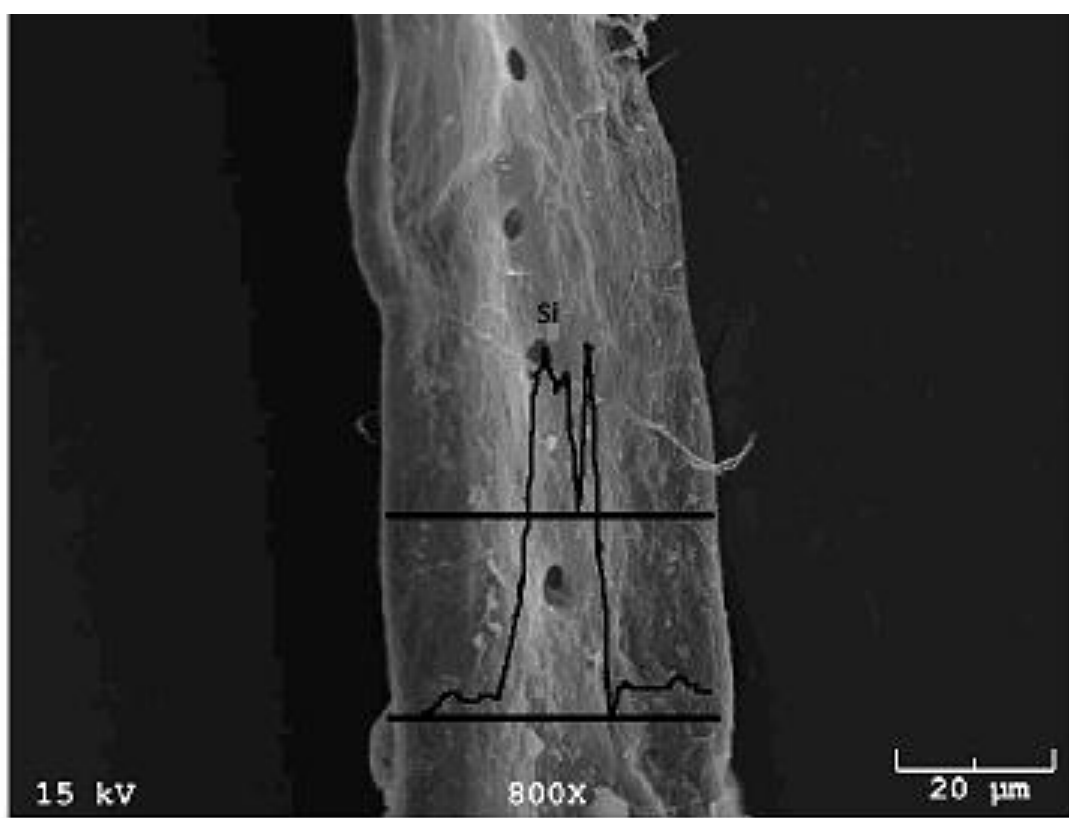


Fig. 3. SEM-EDX line scan of an organo-nanoclay treated fiber

Moisture Absorption

Water molecules can be adsorbed directly by the hydroxyl groups on the external and internal fiber surfaces, including both amorphous and crystallites regions (Okabayashi *et al.* 2004). After the organo-nanoclay treatment, fiber surfaces were covered by hydrophobic organo-nanoclays (as shown in Fig. 2b). As discussed earlier, the organo-nanoclays decreased the accessibility of moisture/water to the fiber surfaces. Reduced accessibility of moisture/water to the hydrophilic groups on the treated fibers would in addition result in a smaller degree of swelling of the fibers to further lower the amount of moisture/water absorption. In fact, swelling of the fiber cell wall is one of main factors contributing to the high degree of moisture absorption in cellulosic fibers.

As can be seen from Fig. 4, the organo-nanoclay treated fibers absorbed about 30% less moisture at saturation, based on the normalized moisture absorption. The normalization is done by dividing the amount of moisture absorbed by the weight of the fiber fraction only to account for the fact that the untreated fibers have no clay. In addition, the slopes of the absorption curves for the treated fibers were lower than that of the untreated fibers for time intervals below 1 hour, suggesting that the absorption rate was also reduced for organo-nanoclay treated fibers. However, the treated fibers still had around 8% to 10% of moisture in the plateau region. Possible causes could include: i) moisture may be absorbed by capillary effect wicking through the clay-clay and clay-fiber interfaces and fiber lumen; ii) some areas of the fiber surfaces were not covered by the organo-nanoclay, since deposition was found to be non-uniform. It is worth noting that after the treatment, the fibers became fluffy and did not form aggregated fiber bundles like the untreated fibers.

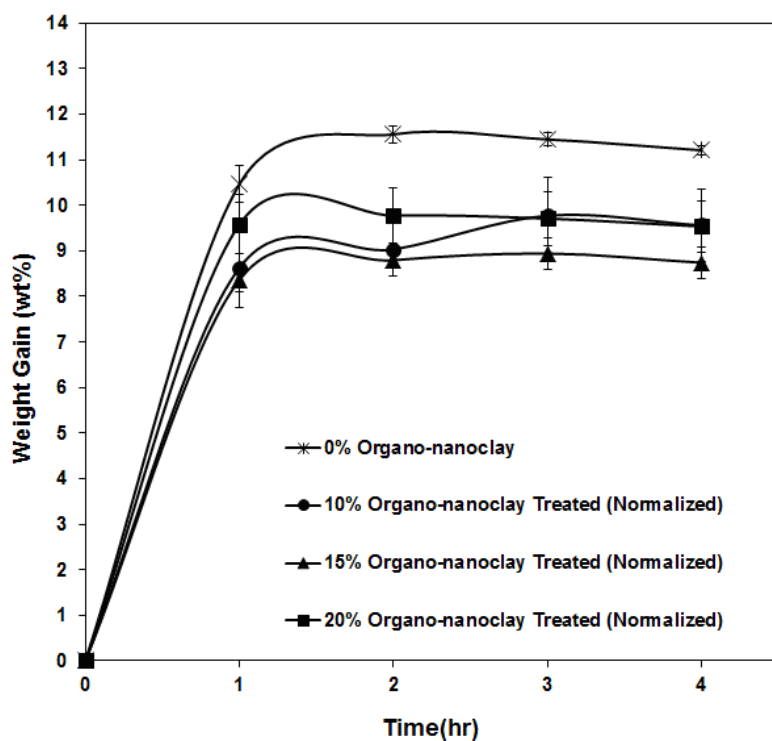


Fig. 4. Comparison of moisture absorption of fibers treated in suspensions of different organo-nanoclay concentrations (wt.%)

It is also interesting to note that the fibers treated in 15-wt% of organo-nanoclays in toluene solution had the lowest amount of moisture absorption. This observation differs from the expectation that higher concentrations of clay adsorption would lead to lesser moisture absorption since more fiber surfaces would have been covered by the hydrophobic clays. This unexpected result could be attributed to the poor exfoliation of the organo-nanoclays at higher concentrations (Yoon *et al.* 2007). If large particles, instead of exfoliated nano-platelets, were deposited on the fiber surfaces, even with a larger amount, the extent of surface coverage by the clays would not increase. Also larger particles might be too big to pass through the fiber pit to cover the internal surface in the lumen. In this study, 15-wt% was chosen as the optimum concentration for fiber treatment in further experiments.

Amount of Water Uptake

Wood fibers are hygroscopic in nature. The results of water uptake amount of the 15-wt% organo-nanoclay treated and untreated fibers after submerging in water are shown in Fig. 5. For the untreated fibers, after 5 minutes, the amount of water uptake was already near saturation. However, for the clay-treated fibers, the water uptake process was much slower.

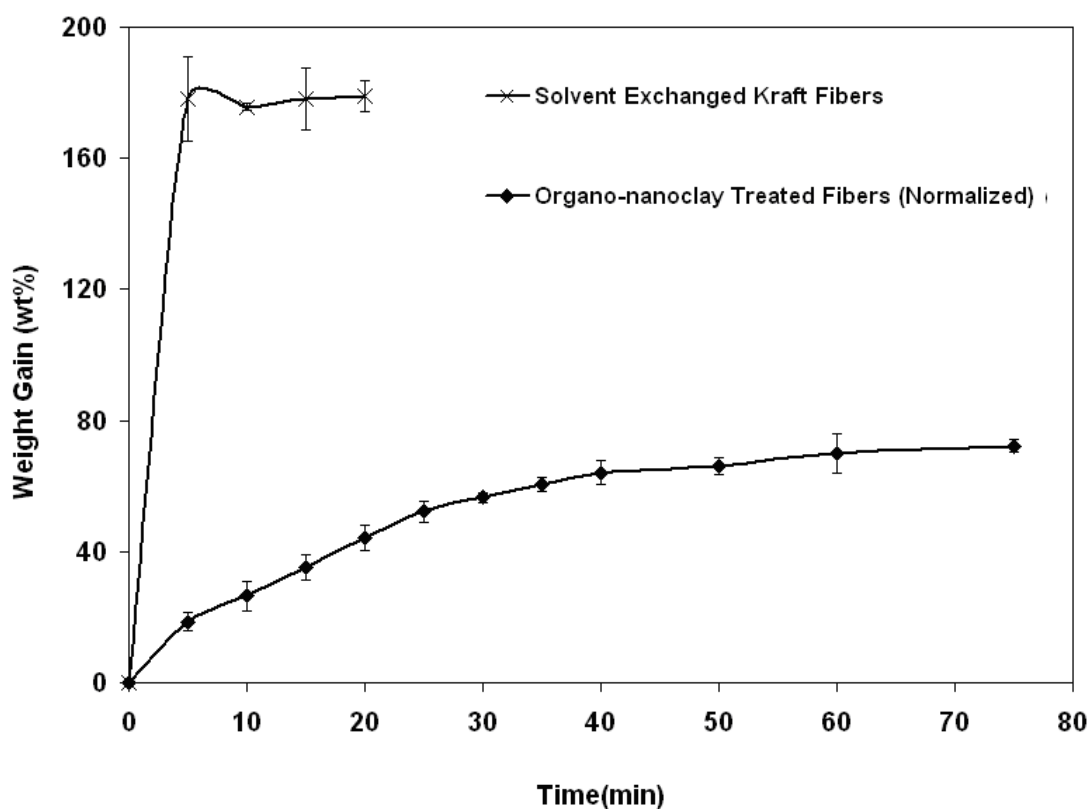


Fig. 5. Weight gain due to water uptake of organo-nanoclay treated and untreated fibers. The data for the treated fibers have been normalized based on the fiber oven-dry weight (g).

After approximately 60 minutes, water uptake of the clay-treated fibers just approached saturation. In addition, clay-treated fibers absorbed a much smaller amount of water (around 120% less) than the untreated fibers upon saturation. Therefore, in addition to blocking the access of water molecules to both internal and external fiber surfaces, the use of organo-nanoclay may have also produced a more tortuous pathway for water to transport to the fiber surfaces (Nah *et al.* 2002; Wu *et al.* 2003). In addition, clay particles will absorb a small amount of moisture as well (given in Table 1). In the untreated fibers, fiber will also swell upon absorption of moisture to promote even more water uptake. Moreover, in the treated fibers, fiber lumens can have a significant amount of organo-nanoclays to reduce the amount of the overall fiber absorption of water at saturation.

Water Contact Angle

Water contact angle reflects surface hydrophobicity. Higher hydrophobicity is signified by a larger water contact angle. When water was dropped on the untreated fiber surfaces, it was absorbed fully within seconds. After the organo-nanoclay treatment, water droplets stayed on the treated fiber mat surface and a contact angle of 164° was achieved (as shown in Fig. 6). This large contact angle indicated that surface hydrophobicity was greatly enhanced. An image of an almost intact water droplet left for 45 minutes on the treated fiber surface is also shown in Fig. 7. The water droplet in Fig. 7 is smaller than the one imaged in Fig. 6 due to evaporation and a small amount of absorption by fiber. An increase in surface roughness was observed due to the water absorption. However, even after 45 minutes, the surface is visibly highly hydrophobic. As shown in Fig. 2, the clay layer on the treated fiber surfaces had a nano-scale roughness and that could have contributed to the high hydrophobicity of the fiber (Youngblood and McCarthy 1999; Callies and Quere 2005).

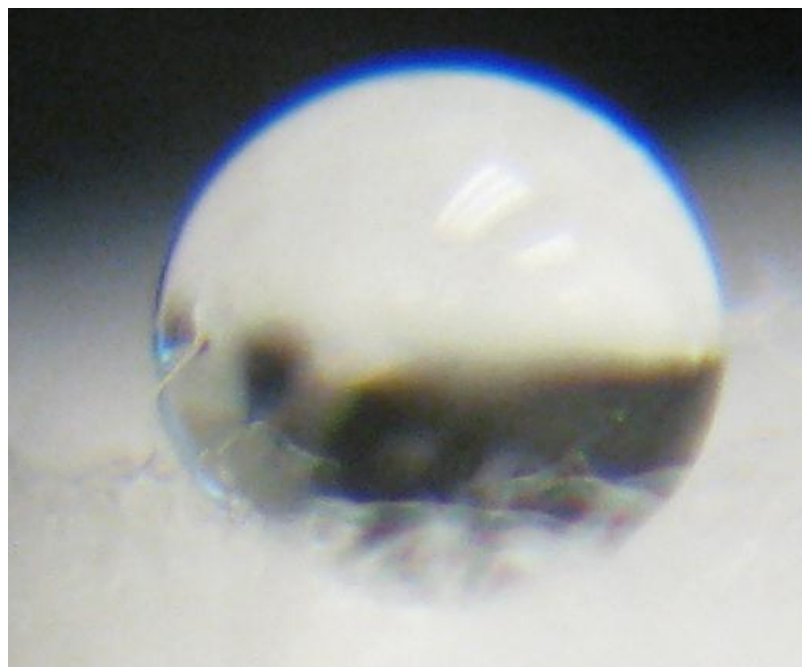


Fig. 6. Water droplet on organo-nanoclay treated kraft fiber mat, after sitting at the surface for 1 minute

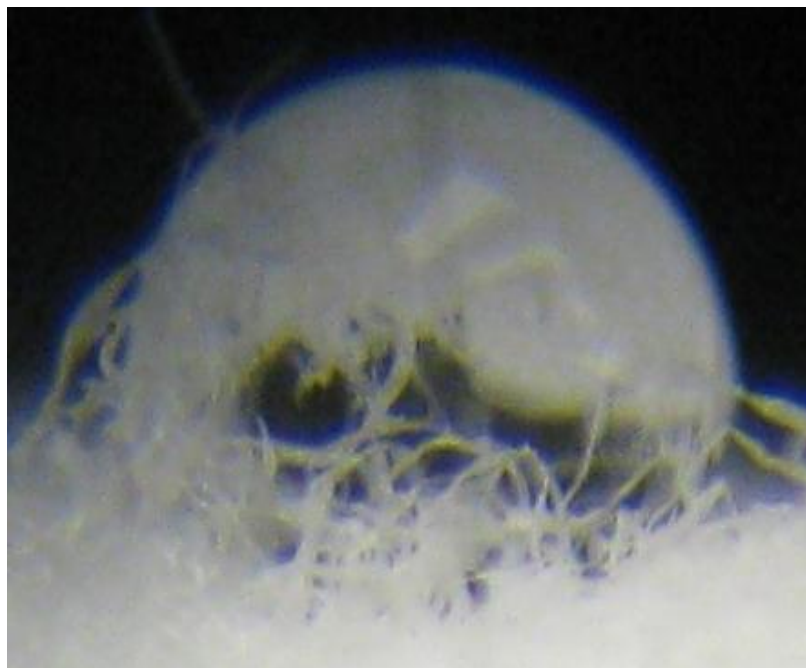


Fig. 7. Water droplet on the treated kraft fiber mat, after sitting at the mat surface for 45 minutes

Surface Energy of Fibers

The DCSE of the organo-nanoclay treated fibers, solvent-exchanged fibers, and untreated fibers was measured using IGC. The results are summarized in Table 3. The DCSE of the organo-nanoclay treated fibers decreased by more than 30% compared with that of the untreated fibers. The solvent-exchanged fibers had a much higher DCSE than the treated fibers but were similar to the untreated fibers. If the total surface energy ($\gamma_s = \gamma^d + \gamma^p$) were considered, the decrease in the surface energy of the organo-nanoclay treated fibers would have been even larger because of the expected decrease in the polar component of the surface energy, which is not measured by the IGC experiment (TZE and Gardner 2001). The DCSE of all samples decreased when temperature was increased from 60°C to 80°C.

Table 3. The Influence of Clay Treatment on DCSE of the Fibers

Sample Type	Surface Energy DCSE@ 60°C (mJ/m ²)	DCSE @70°C (mJ/m ²)	DCSE@ 80°C (mJ/m ²)
Untreated fibers	45.96(1.22)	43.70(1.04)	43.14(1.58)
Solvent exchanged fibers	44.39(0.64)	42.83(0.82)	41.25(1.35)
Organo-nanoclay treated fibers	30.26(1.17)	29.44(1.12)	27.57(0.97)

Note: the data in the parentheses are the standard deviation.

Thermal Stability of the Treated Fibers

Thermal stability of the organo-nanoclay treated fibers as measured by TGA was compared to the solvent-exchanged and untreated fibers in Fig. 8. There appeared to be two main regions in the fiber thermal degradation process. The first region was at the temperature of 100°C or lower. In this temperature range, the weight loss was mostly attributable to water evaporation. The second region of major weight loss started at around 300°C and corresponded to a loss of structural hydroxide groups in combination with other thermal decomposition reactions (Yoon *et al.* 2007). It has been reported that the organo-nanoclays could act as a barrier to hinder the diffusion of heat and migration of degraded volatiles at weight loss lower than 5% (Liu *et al.* 2011; Lin *et al.* 2008; Cerruti *et al.* 2008; Wan *et al.* 2004). The thermal characteristics, including 5% weight loss temperature (based on the dry fiber weight), maximum degradation rate, and temperature at maximum degradation rate, are summarized in Table 4. The results showed that thermal stability of the treated fibers was not significantly affected by the modification procedure.

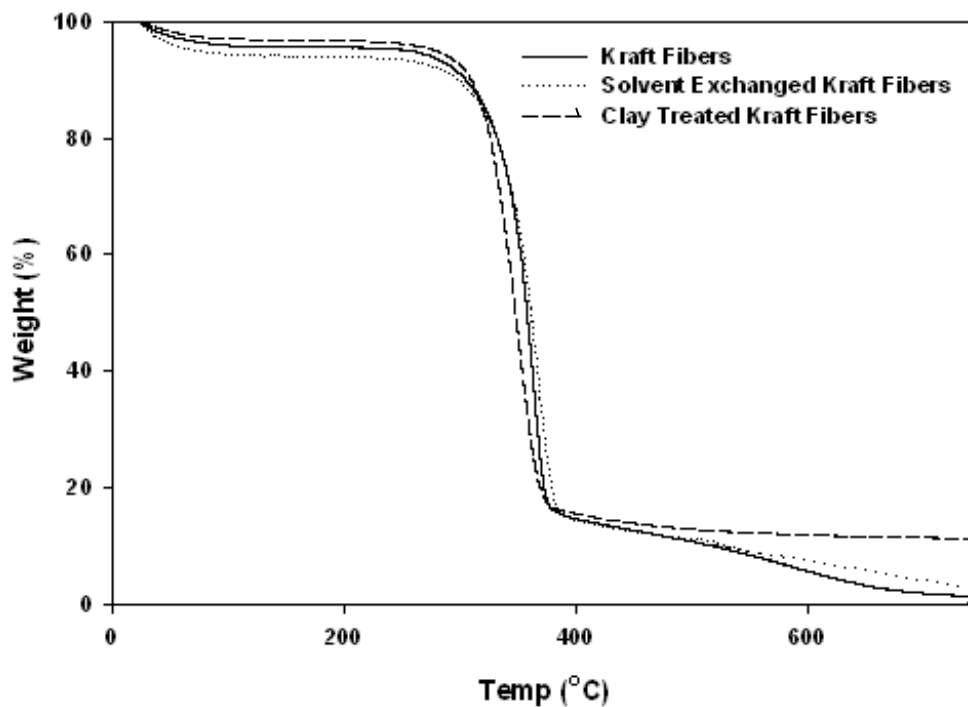


Fig. 8. TGA weight degradation curves of the treated and untreated fibers

Table 4. Thermal Characteristics of the Fibers

Fibers	Temp. at 5% wt. loss	Max. deg. rate (%/°C)
Untreated Fibers	301	2.2
Solvent Exchanged Fibers	299	1.8
Clay Treated Fibers	304	1.4

FTIR Analysis

The fibers were analyzed using FTIR to identify their functional groups (Fig. 9). Some of the obvious differences in the spectra of organo-nanoclay treated fibers are Si-O stretching bands at 800 cm^{-1} , 520 cm^{-1} , and 462 cm^{-1} (Nayak and Singh 2007). There are three types of hydrogen bonds (two intra-cellulose and one inter-cellulose) at the broad OH stretching band located around 3600 to 3000 cm^{-1} (Oh *et al.* 2005). For the solvent-exchanged fibers, these types of hydrogen bonding were at 3404 cm^{-1} , 3373 cm^{-1} , and 3356 cm^{-1} . But for the organo-nanoclay treated fibers, one of the peaks shifted from 3373 cm^{-1} to a higher wave number of 3381 cm^{-1} . This peak shift indicated that there might be new hydrogen bonds formed between the hydroxyl groups of the fibers and that of the organo-nanoclays, which could be one reason why organo-nanoclays could be attached to the fiber surfaces.

According to published literature (Oh *et al.* 2005), the relative absorbance ratio ($A_{4000-2995}/A_{897}$) represents hydrogen bonding intensity. It can be seen from Table 5 that the hydrogen bonding intensity of the organo-nanoclay treated fibers was much lower than that of the original fibers (less than half), and slightly lower than that of the solvent-exchanged fibers. This implied that fewer hydrogen bonds were formed in the fibers that were solvent-exchanged and/or organo-nanoclays treated.

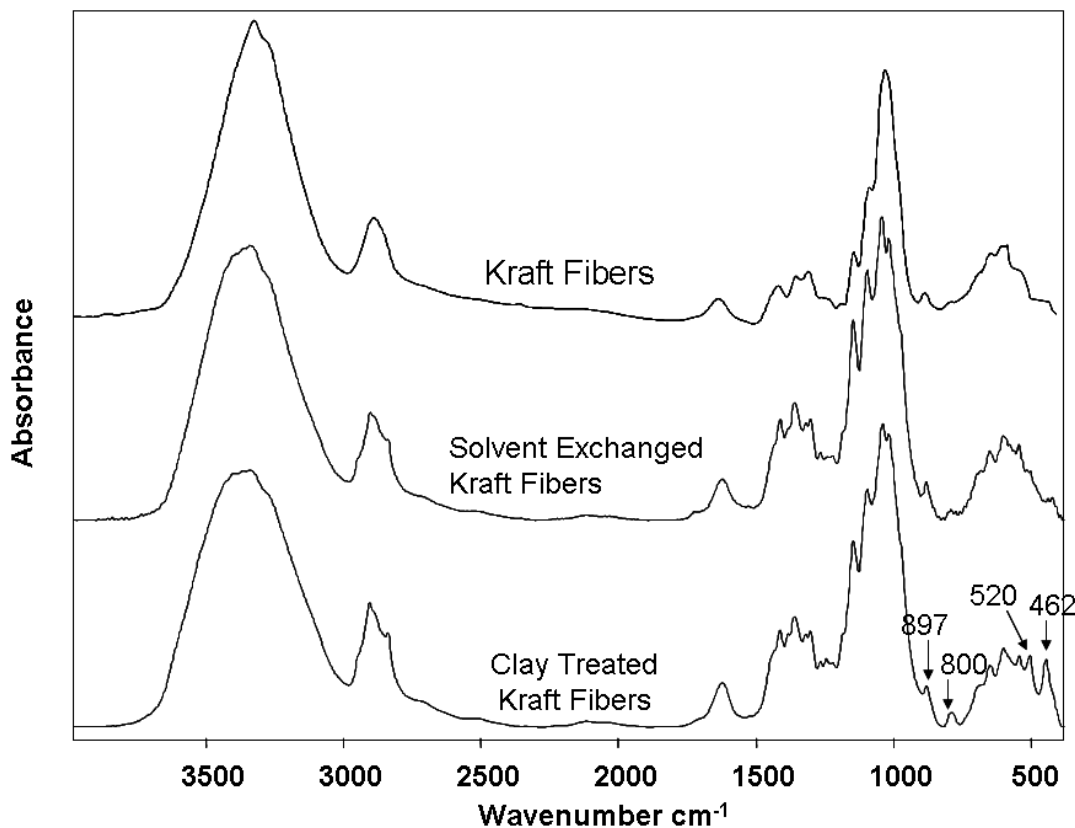


Fig. 9. FTIR spectra of untreated, organo-nanoclay treated, and solvent-exchanged kraft fibers

Table 5. The Calculated Relative Absorbance Ratio of A₄₀₀₀₋₂₉₉₅/A₈₉₇

Samples	A ₄₀₀₀₋₂₉₉₅	A ₈₉₇	A ₄₀₀₀₋₂₉₉₅ /A ₈₉₇
Untreated fibers	95.92	0.49	196.96
Solvent Exchanged Fibers	92.04	1.10	83.67
Clay Treated Fibers	96.85	1.17	76.26

In addition to hydrogen bonding, there might be other interactions, such as electrostatic forces, acting between the fiber surfaces and organo-nanoclays. The surface charge of the organo-nanoclay Cloisite 93A in toluene was tested using a Zeta Potential Analyzer (Brook Heaven Instrument Cooperation, USA). It was found that zeta potential was around 43 mV, indicating that the organo-nanoclays were positively charged in toluene. Zeta potential of the solvent-exchanged fibers could not be tested in toluene because of their poor dispersion. If the solvent-exchanged kraft fibers were still negatively charged, like the untreated fibers in water, then Cloisite 93A could also be attached to the kraft fiber surface by electrostatic forces. The multilayer adsorption of the organo-nanoclays to the fiber surface, as shown by the TEM image, could be one of the indications for the existence of electrostatic adsorption.

CONCLUSIONS

1. In this study, it was found that organo-nanoclay treatment of kraft pulp fibers using a solvent-exchange process increased fiber surface hydrophobicity. The organo-nanoclay treatment significantly reduced the amount of moisture absorption and water uptake amount (submersion in water) of the fibers. The contact angle of water on the treated fiber mat was very high at 164° and remained high for 45 minutes after droplet placement at room temperature.
2. The TEM images showed that the adsorbed organo-nanoclays on the fiber surface had multilayer characteristics. It was also shown by SEM-EDX scans that some organo-nanoclays could have entered into the fiber lumen. FTIR results suggested the formation of additional hydrogen bonding between the nanoclay particles and the solvent-exchanged fiber surfaces, and it also revealed a decrease of hydrogen bonding in the treated fibers.
3. The DCSE of treated kraft pulp fibers decreased and the DCSE of all the fibers treated or untreated decreased with the increase of temperature from 60 °C to 80 °C. The organo-nanoclay treated fibers had similar thermal stability as the untreated fibers.

ACKNOWLEDGMENTS

Financial support by the Early Researcher Award from Ontario Ministry of Research and Innovation and NSERC ForValueNet Strategic Network is greatly appreciated.

REFERENCES CITED

- Balu, B., Breedveld, V. and Hess, D. W. (2008). "Fabrication of "roll-off" and "sticky" superhydrophobic cellulose surfaces via plasma processing," *Langmuir* 24(1), 4785-4790.
- Bessadok, A., Marais, S., Gouanve, F., Colasse, L., Zimmerlin, I., Roudesli, S. and Metayer, M. (2007). "Effect of chemical treatments of Alfa (*Stipa tenacissima*) fibers on water-sorption properties," *Compos. Sci. Technol.* 67(3-4), 685-697.
- Callies, M. and Quere, D. (2005). "On water repellency," *Soft Matter* 1, 55-61.
- Cerruti, P., Ambrogi, V., Postiglione, A., Rychly, J., Matisova-Rychla, L. and Carfagna, C. (2008), "Morphological and thermal properties of cellulose-montmorillonite nanocomposites," *Biomacromolecules* 9, 3004-3013.
- Choudalakis, G. and Gotsis, A. D. (2009). "Permeability of polymer/clay nanocomposites: A review," *Eur. Polym. J.* 45(4), 967-984.
- Clapperton, R. H. and Henderson, W. (1947). *Modern Paper-Making*. 3rd Ed., Basil Blackwell, Oxford, p. 120.
- Goncalves, G., Marques, P., Trindade, T., Neto, C. P. and Gandini, A. (2008). "Superhydrophobic cellulose nanocomposites," *J. Colloid Interface Sci.* 324, 42-46.
- Hu, Z., Zen, X., Gong, J. and Deng, Y. (2009). "Water resistance improvement of paper by superhydrophobic modification with micro-sized CaCO₃ and fatty acid coating," *Colloids Surf. A* 351, 65-70.
- Ishida, Y., Ohtani, H., Tsuge, S. and Yano, T. (1994). "Determination of styrene copolymer sizing agents in paper by pyrolysis gas chromatography," *Anal. Chem.* 66(9), 1444-1447.
- Jin, C., Yan, R., and Huang, J. (2011). "Cellulose substance with reversible photo-responsive wettability by surface modification," *J. Mater. Chem.* 21, 17519-17525.
- Khalil, H., Ismail, H., Rozman, H. D. and Ahmad, M. N. (2001). "The effect of acetylation on interfacial shear strength between plant fibers and various matrices," *Eur. Polym. J.* 37(5), 1037-1045.
- Kim, J. K., Hu, C., Woo, R. S. C. and Sham, M. L. (2005). "Moisture barrier characteristics of organoclay-epoxy nanocomposites," *Compos. Sci. Technol.* 65(5), 805-813.
- Lei, Y., Wu, Q., Clemons, C. M., Yao, F., and Xu, Y. (2007). "Influence of nanoclay on properties of HDPE/wood composites," *J. Appl. Polym. Sci.* 106(6), 3958-3966.
- Li, S., Wei, Y., and Huang, J. (2010). "Facile fabrication of superhydrophobic cellulose materials by a nanocoating approach," *Chem. Lett.* 39, 20-21.
- Lin, Z., Renneckar, S., and Hindman, D. P. (2008). "Nanocomposite-based lignocellulosic fibers 1. Thermal stability of modified fibers with clay-polyelectrolyte," *Cellulose* 15, 333-346.

- Lindstrom, T., Banke, K., Larsson, T., Glad-Nordmark, G., and Boldizar, A. (2008). "Nanoclay plating of cellulosic fiber surfaces," *J. Appl. Polym. Sci.* 108, 887-891.
- Liu, A., Walther, A., Ikkala, O., Belova, L. and Berglund, L. A. (2011). "Clay nanopaper with tough cellulose nanofiber matrix for fire retardancy and gas barrier functions," *Macromolecules* 12, 633-641.
- Nah, C., Ryu, H. J., Kim, W. D. and Choi, S. S. (2002). "Barrier property of clay/acrylonitrile-butadiene copolymer nanocomposites," *Polym. Adv. Technol.* 13, 649-652.
- Nakajima, A., Hashimoto, K., and Watanabe, T. (2001). "Recent studies on superhydrophobic films," *Monatsh. Chem.* 132(1), 31-41.
- Nayak, P. S., and Singh, B. K. (2007). "Instrumental characterization of clay by XRF, XRD and FTIR," *Bull. Mater. Sci.* 30(3), 235-238.
- Nystrom, D., Lindqvist, J., Ostmark, E., Antoni, P., Carlmark, A., and Hult, A. (2009). "Superhydrophobic and self-cleaning bio-fiber surfaces via ATRP and subsequent postfunctionalization," *ACS Appl. Mater. Interfaces* 1(4), 816-823.
- Nystrom, D., Lindqvist, J., Ostmark, E. and Hult, A. (2006). "Superhydrophobic biofiber surfaces via tailored grafting architecture," *Chem. Commun.* 34, 3594-3596.
- Oh, S. Y., Yoo, D., Shin, Y., and Seo, G. (2005). "FTIR analysis of cellulose treated with sodium hydroxide and carbon dioxide," *Carbohydr. Res.* 340, 417-428.
- Okabayashi, S., Griesser, U. J., and Bechtold, T. (2004). "A kinetic study of moisture sorption and desorption on lyocell fibers," *Carbohydr. Polym.* 58, 293-299.
- Peeterbroeck, S., Alexandre, M., Jerome, R. and Dubois, P. (2005). "Poly (ethylene-co-vinyl acetate)/clay nanocomposites: Effect of clay nature and organic modifiers on morphology, mechanical and thermal properties," *Polym. Degrad. Stab.* 90, 288-294.
- Quan, C., Werner, O., Wågberg, O., and Turner, J. (2009). "Generation of superhydrophobic paper surfaces by a rapidly expanding supercritical carbon dioxide-alkyl ketene dimer solution," *J. Supercrit. Fluids* 49(1), 117-124.
- Tze, W. T. and Gardner, D. J. (2001). "Contact angle and IGC measurements for probing surface-chemical changes in the recycling of wood pulp fibers," *J. Adhes. Sci. Technol.* 15(2), 223-241.
- Wan, C., Tian, G., Cui, N., Zhang, Y., and Zhang Y. (2004). "Processing thermal stability and degradation kinetics of poly (vinyl-chloride)/montmorillonite composites," *J. Appl. Polym. Sci.* 92(3), 1521-1526.
- Wu, Y., Jia, Q., Yu, D., and Zhang, L. (2003). "Structure and properties of nitrile rubber (NBR)-clay nanocomposites by co-coagulating NBR latex and clay aqueous suspension," *J. Appl. Polym. Sci.* 89(14), 3855-3858.
- Yang, H., and Deng, Y. (2008). "Preparation and physical properties of superhydrophobic papers," *J. Colloid Interface Sci.* 325, 588-593.
- Yang, N., and Deng, Y. (2000). "Paper sizing agents from micelle-like aggregates of polystyrene-based cationic copolymers," *J. Appl. Polym. Sci.* 77(9), 2067-2073.

- Yoon, K., Sung, H., Hwang, Y., Noh, S. K., and Lee, D. (2007). "Modification of montmorillonite with oligometric amine derivatives for polymer nanocomposite preparation," *Appl. Clay Sci.* 38, 1-8.
- Youngblood, J. P., and McCarthy, T. J. (1999). "Ultrahydrophobic polymer surfaces prepared by simultaneous ablation of polypropylene and sputtering of poly (tetrafluoroethylene) using radio frequency plasma," *Macromolecules* 32, 6800-6806.
- Zhang, X., and Shi, F. (2008). "Superhydrophobic surfaces: From structural control to functional application," *J. Mater. Chem.* 18(6), 621-633.

Article submitted: April 16, 2012; Peer review completed: May 28, 2012; Revised version received: July 14, 2012; Accepted: July 16, 2012; Published: July 20, 2012.